Ultra-Fast Silicon Detectors (UFSD)

H. F.-W. Sadrozinski*, A. Anker, J. Chen, V. Fadeyev, P. Freeman, Z. Galloway, B. Gruey, H. Grabas, C. John, Z. Liang, R. Losakul, S. N. Mak, C. W. Ng, , A. Seiden, N. Woods, A. Zatserklyaniy
SCIPP, Univ. of California Santa Cruz, CA 95064, USA
B. Baldassarri, N. Cartiglia, F. Cenna, M. Ferrero
Univ. of Torino and INFN, Torino, Italy
G.Pellegrini, S. Hidalgo, M. Baselga, M. Carulla, P. Fernandez-Martinez, D. Flores, A. Merlos, D. Quirion
Centro Nacional de Microelectrónica (CNM-CSIC), Barcelona, Spain
M. Mikuž, G.Kramberger, V. Cindro, I. Mandić, M. Zavrtanik
IJS Ljubljana, Slovenia

Abstract– We report on measurements on Ultra-Fast Silicon Detectors (UFSD) which are based on Low-Gain Avalanche Detectors (LGAD). They are n-on-p sensors with internal charge multiplication due to the presence of a thin, low-resistivity diffusion layer below the junction, obtained with a highly doped implant. We have performed several beam tests with LGAD of different gain and report the measured timing resolution, comparing it with laser injection and simulations. For the 300µm thick LGAD, the timing resolution measured at test beams is 120ps while it is 57ps for IR laser, in agreement with simulations using Weightfield2. For the development of thin sensors and their readout electronics, we focused on the understanding of the pulse shapes and point out the pivotal role the sensor capacitance plays.

PACS: 29.40.Gx, 29.40.Wk, 78.47jc
Keywords: fast silicon sensors; charge multiplication; thin tracking sensors; silicon strip; pixel detectors.

1 Introduction

We propose an ultra-fast silicon detector that would establish a new paradigm for space-time particle tracking [1]. Presently, precise tracking devices determine time quite poorly while good timing devices are too large for accurate position measurement. We plan to develop a single device that ultimately will measure with high precision concurrently the space (~10 µm) and time (~10 ps) coordinates of a particle.

First applications of UFSD are envisioned in LHC upgrades, in cases where the excellent time resolution coupled with good spatial resolution helps to reduce drastically pile-up effects due to the large number of individual interaction vertices. While ATLAS is proposing UFSD as one of the technical options for the High Granularity Timing Detector (HGTD) located in front of the forward calorimeter (FCAL), CMS-TOTEM are considering UFSD to be the timing detectors for the high momentum - high rapidity Precision Proton Spectrometer (CT-PPS), residing in Roman-pots about 200 m from the interaction region. In both cases, the UFSD would be of moderate segmentation (a few mm^2) with challenging radiation requirements (few times 10^{15} neq/cm^2), requiring a time resolution of 30ps, which could be achieved by stacking up in series up to four sensors.

UFSD are thin pixelated n-on-p silicon sensors based on the LGAD design [2], [3] developed by CNM Barcelona. The LGADs exhibit moderate internal gain (~10x) due to a highly doped p+ region just below the n-type implants. Based on the progress made through 7 fabrication cycles, the performance of LGAD have been established in several beam tests and with laser laboratory measurements. The sensors tested were routinely operated for long time periods at an operating bias voltage close to 1000V for 300 µm thickness (500V for 50 µm) and various internal gains of 3 to 20.

Since present experience with LGAD is limited to sensors with 300 µm thickness [4], a reliable tool is needed to extrapolate their performance to the planned thickness of 50 µm. This is done with the simulation program *Weightfield2* (WF2) [5] that has been developed specifically for the simulation of the charge collection in semiconductors. In the following, we compare the pulse shapes of thick and thin LGAD to elucidate the advantage of thin sensors, including those due to trapping effects after irradiation. This is followed by an introduction to precision timing in silicon detectors and a prediction of the expected timing resolution as a

* Corresponding author, hartmut@ucsc.edu, Tel: (831) 459 4670, Fax:(831) 459 5777

function of LGAD thickness and internal gain. The predictions will be confronted with results from several beam tests and laboratory laser measurements. Finally we present pulse shapes on thin LGADs and the pivotal role the sensor capacitance plays in the timing resolution of UFSD.

2 LGAD PULSE SHAPES

The *Weightfield2* program [5] simulates the electrostatic fields and the charge collection in LGAD, including the effect of the internal gain. The current output of the sensor can then be convoluted with the response of the front-end electronics generating a voltage signal that can be used to evaluate the timing capabilities of a detector. Figure 1.a shows the output current for a minimum ionizing particle (MIP) traversing a 50 µm thick LGAD with gain 10 biased at large over-depletion, showing the separate contributions from the drift of both the initial and gain electrons and holes, respectively. For thicker LGAD, the current pulse has the same shape as that shown in the picture, with the only difference that the pulse duration is scaled by the thickness, i.e. the 1ns collection time for the 50 µm thick LGAD becomes 9 ns for 300 µm thickness. In Fig.1.b the voltage signals from a broad-band amplifier (BB) are shown for LGADs of different thickness, indicating that for constant gain the maximum pulse height is independent of the LGAD thickness, and that the shorter rise time favors the thin sensor for timing application.

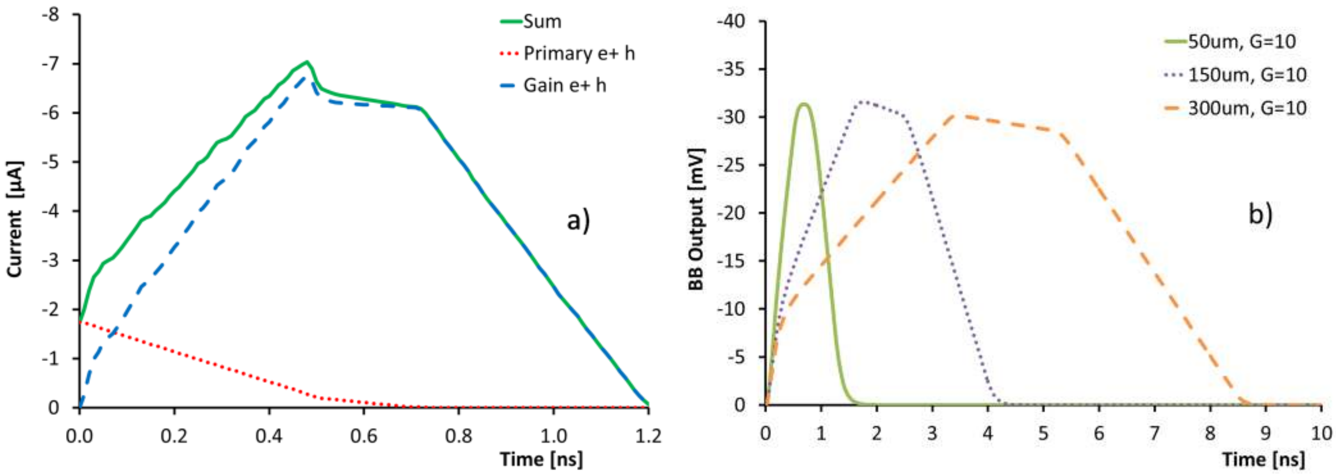

Fig. 1 Pulse shapes of LGAD simulated with WF2 version 3.5: a) detector current for a MIP traversing a 50 µm thick LGAD; b) voltage output from a x100 broad-band amplifier (BB) with 50Ω input for LGADs with gain of 10 and thickness 50, 150, 300µ [5].

The change of the LGAD pulse shape due to trapping after irradiation can be studied with WF2, of which version 3.5 incorporates trapping [6]. Since the characteristic trapping time is about 0.5 ns (corresponding to a trapping length of ~ 50 µm), on comparing the signals from thin and thick detectors shown in Fig 1.b one would expect that the longer pulses of thick detector will be effected much more by trapping than the short ones from thin LGAD. This is illustrated in Fig. 2 where the BB pulses for LGAD with gain 10 and thickness a) 300 µm and b) 50 µm, respectively, (note the different time scale) are shown for different neutron fluences. For 300 µm LGAD (Fig. 2.a), the large loss of gain holes changes the pulse shape drastically and reduces the observed gain (defined as the ratio of pulse areas of LGAD over that of no-gain diodes) by a large amount. The effect of trapping on thin sensors is much less drastic as shown in Fig. 2.b: the pulse shape and the rising edge are preserved (which is good for timing) and the gain loss is limited.

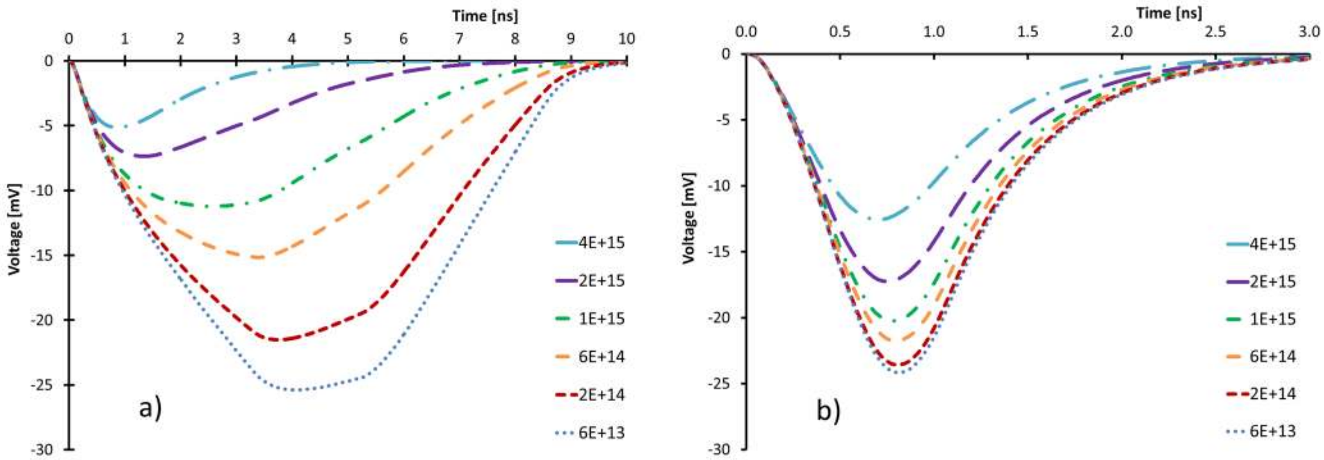

Fig. 2 WF2 simulation of BB pulse shapes of MIP signals due to trapping for different neutron fluences (in units of neq/cm^2) for LGAD of gain 10 with two thickness': a) 300 µm, b) 50 µm. Note the different time scales.

For timing application, the pulse amplitude is more important than the pulse area. The variation of signal amplitude as a function of neutron fluence is shown in Fig. 3 for 300 and 50 µm thick LGADs: up to a fluence of 4*10^{15}, the pulse height loss due to trapping for a 50 µm thick LGAD is less than 50% of its pre-rad value.

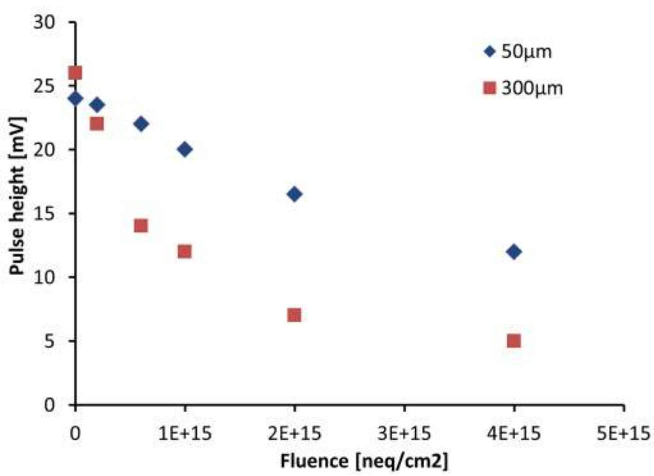

Fig. 3 WF2 simulation of the BB pulse height of MIP signals as function of neutron fluence for LGAD of gain 10 with 50 µm and 300 µm thickness when only trapping is considered.

The mechanisms underlying the radiation effects in LGADs are under intensive investigation within RD50 [7]. Up to now, data are available for 300 µm thick LGAD, and the data are interpreted in terms of a decrease in the gain in addition to the signal decrease caused by trapping at fluences beyond 10^{14} neq/cm^2 [8], This has been identified with an initial acceptor removal, depending on both the boron doping concentration and the interstitial defects created during irradiation [9]. The acceptor removal appears to level off at higher fluences so that a gain of about 3.5 is observed at a fluence of 2*10^{15} neq/cm^2, for which we project a timing resolution of about 60ps, using Figs. 4 and 7 and assuming that the timing resolution scales with dV/dt. We are fabricating thin sensors with a variety of gain values and bulk resistivities for irradiations to verify the acceptor removal model. In addition, we are working on replacing the boron in the multiplication layer by gallium, which has been shown to be more radiation resistant.

3 SIMULATION OF THE UFSD TIMING RESOLUTION

We have used WF2 to simulate LGAD parameters which drive the timing resolution: internal gain, capacitance and thickness. The time resolution σ_t is given by contributions from time walk, jitter and TDC binning:

$$\sigma_t^2 = ([\frac{V_{th}}{dV/dt}]_{RMS})^2 + (\frac{N}{dV/dt})^2 + (\frac{TDC_{bin}}{\sqrt{12}})^2$$

with V_{th} the signal threshold, dV/dt the signal slope or slew-rate, N the noise, and TDC_{bin} the size of a TDC bin, indicating the central role of the slew-rate of the signal dV/dt [10]. This means that we need both large and fast signals. We are still quantifying the contributions to the time resolution due to the non-uniform charge deposition within the sensor caused by local Landau fluctuation (in addition to the standard time-walk contribution), and will report on this issue soon in a separate paper. Using WF2, we can show that the time resolution improves with larger gain as well as with thin detectors (Fig. 4), since both increase the slew-rate. An additional advantage is expected from sensors with reduced capacitance, i.e. small area, as they permit larger slew-rate for a fixed input impedance of the amplifier (see Sec. 5 below).

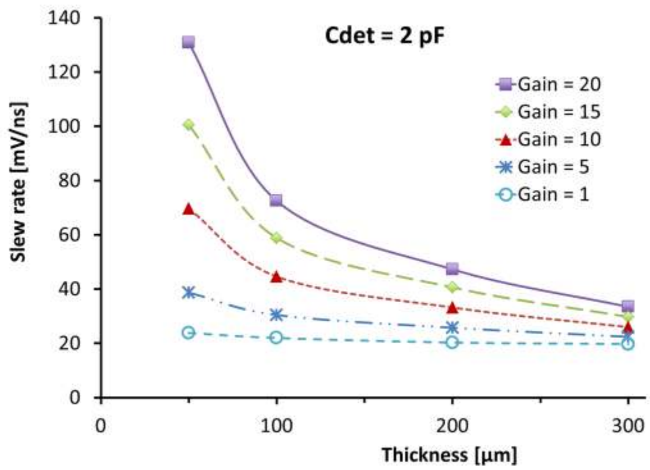

Fig. 4 WF2 simulations of the slew-rate dV/dt as measured by a 50 Ω Broadband amplifier as a function of sensor thickness and various gain values. They indicate the good time resolution achievable with thin LGAD with gain. At 50 µm thickness, a gain of 10 results in a three-fold improvement in the time resolution when compared to a no-gain sensor.

4 TIMING RESOLUTION MEASUREMENTS

We measured the time resolution of 300 µm thick LGAD pads with internal gains between 10 to 20 in the CERN H6 170 GeV pion beam-using sensors with different capacitances (4 pF and 12 pF) [11]. With a view on the upcoming design of the electronics readout, we used several analysis algorithms to optimize the time resolution: (i) a constant low threshold, (ii) the time of the pulse maximum, (iii) an extrapolation of the slope to the base line, and (iv) a constant fraction discriminator (CFD). As an example, Fig. 5 shows the timing resolution and time walk at constant 10 mV threshold as a function of pulse height for a 300 µm thick LGAD. In the region of single MIPs with pulse height between 40 and 80 mV, the timing resolution is between 150ps and 200 ps, and the time walk is substantial at about 400 ps.

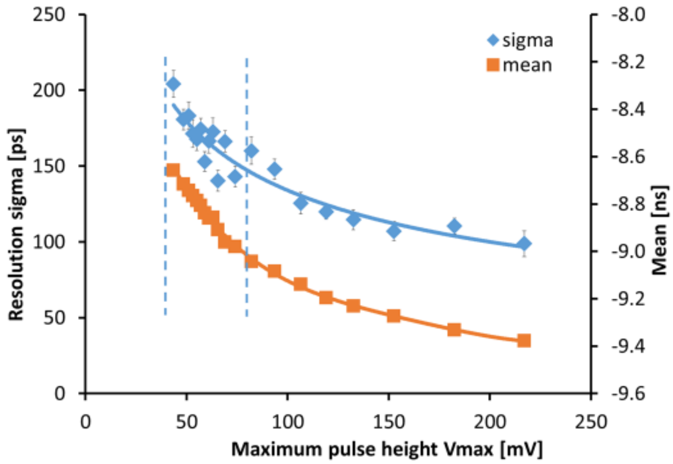

Fig. 5 Timing resolution and time walk of the mean at constant 10 mV threshold for a 300 µm thick LGAD with gain 10 in the Nov. 2014 beam test. The vertical lines indicate the range of a MIP. A running average of 1 ns is used to filter the data [11].

Fig. 6 shows the time resolution for LGADs with different capacitances (12 pF and 4 pF) as a function of CFD threshold for different filter (running average) times of the pulse. The CFD approach is the timing method we found preferable since it eliminates to a great extent the time walk error [11]. As predicted by simulations, reducing the capacitance from 12 pF to 4 pF improves the time resolution by 25%, going from 160 ps to 120 ps for CFD threshold set at 5-15% and applying a low pass filter set at about 500 MHz.

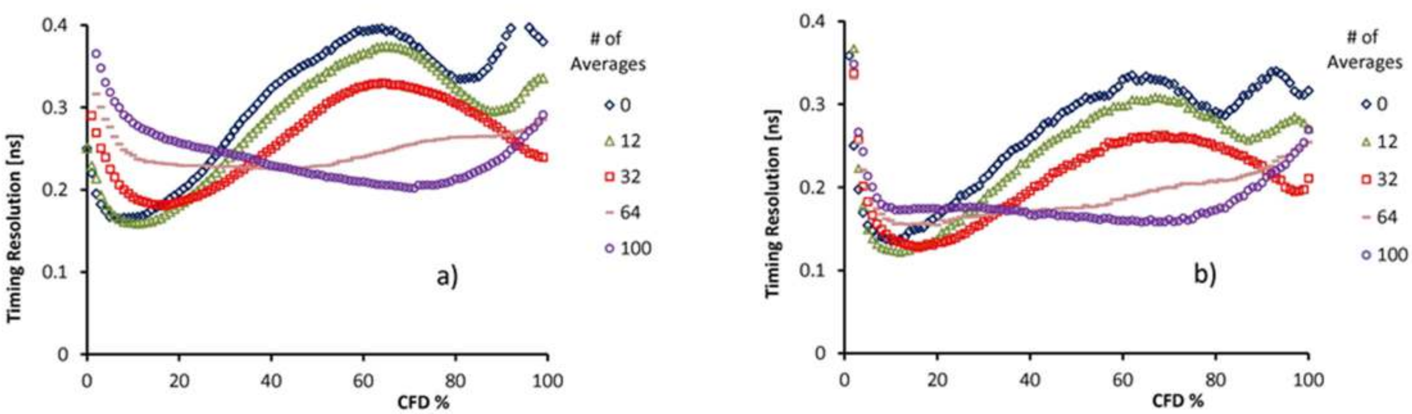

Fig. 6 CFD Time resolution of LGADs with different capacitances: a) 12 pF (left) [11] and b) 4 pF.

Our present understanding of the timing resolution for 300 µm thick LGAD is shown in Fig. 7. Improved resolution is seen for laser vs. beam test data since the laser is not subject to time walk and Landau fluctuations. Another improvement measured and properly predicted is when the LGAD capacitance is reduced. The only measurement not agreeing with the WF2 simulations is the lowest laser measurement at 300 µm. The fact that it is lower than the WF2 prediction is traced to an improved noise behavior of the measurement not captured in the simulations [10]. The good agreement of the measured time resolution from both laser measurements (only time jitter) and beam tests (time jitter, time walk and Landau fluctuations) with the WF2 simulation justifies the extrapolation of the expected time resolution to thinner sensors (Fig. 7). For a 50 µm thick LGAD with gain of 10 we expect a time resolution of 30 ps.

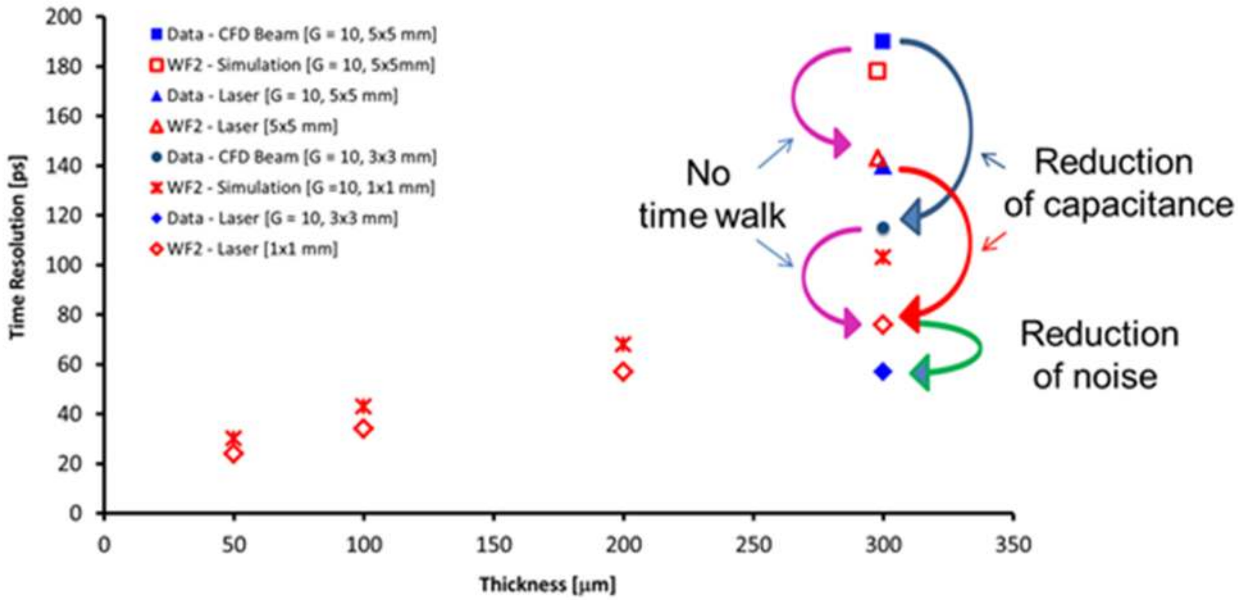

Fig. 7 Time resolution for LGADs with gain of 10 as a function of sensor thickness, combining both test beam and laser measurements (at 300 μm) –closed symbols- with WF2 simulations –open symbols-.

5 Thin LGAD

Thin LGAD were produced on 100 Ω-cm epitaxial p-type wafers with different pad areas, and used to investigate the effect of the capacitance on the output pulses. Figure 8 shows the results of measurements on two 50 μm thick pads: the $1/C^2$ curve (fig. 8.a) indicates a depletion voltage of 170V and the capacitances to be 2.6 pF for the small diode SD2 of area 1mm x 1mm and 35 pF for the large diode BD3 of area 4mm x 4mm. It also shows the "voltage lag" at low voltages typical for LGAD accounting for the depletion of the gain layer. When the C-V data are used to extract the doping concentration (Fig. 8.b), the epi LGADs show a lower value of the gain layer doping with respect to what has been seen in previous float zone LGAD with gain of 15 and 7, respectively [4]. The measured gain of 3.5 using IR laser shown in Fig. 8.c is consistent with the doping profile and with the relatively small voltage lag of Fig. 8.a. The data show a bias voltage range of 500V, very large for the thin sensors.

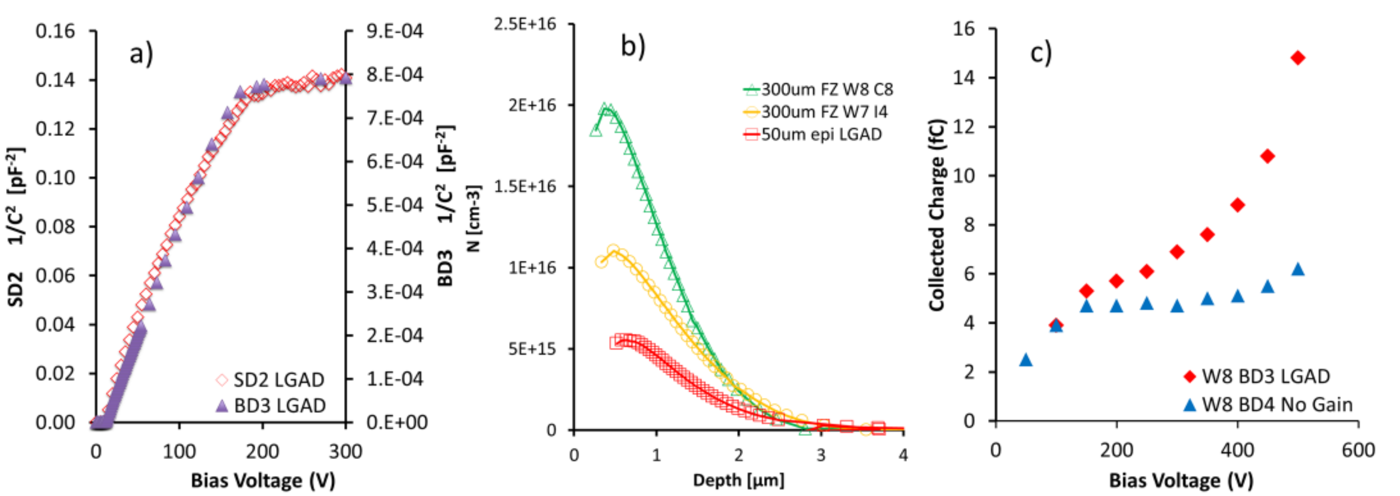

Fig. 8 Measurement results on 50 μm thick epitaxial LGAD: a) C-V measurement showing a relatively small "voltage lag" at low bias; b) doping profile extracted from C-V for FZ and epi LGAD indicating lower doping concentration in the multiplication layer for the epi LGAD; c) comparison of charge collection in IR laser injection on epi LGAD and no-gain diode yielding a gain of 3.5 for the LGAD.

Our measurement is performed using a broad-band amplifier of fixed 50 Ω input impedance; for our analysis we need to properly take into account the effect of the sensor capacitance C. A first important effect is that the capacitance of the LGADs has a strong influence on the pulse shapes: see Fig. 9.a for pulse shapes taken with α particles injected from the front of the sensors together with the corresponding simulated WF2 pulses. The simulated WF2 data shown are displayed on a vertical scale which has been properly adjusted to take into account the gain of the amplifier and the fraction of the α energy absorbed in the sensitive part of the LGAD, about 50%, as determined from the collected charge. Compared to a LGAD with C=35 pF, the small LGAD with C = 2.6 pF exhibits a 3-fold increase in amplitude and a 5-fold increase in the slew rate dV/dt as seen in Fig. 9.b.

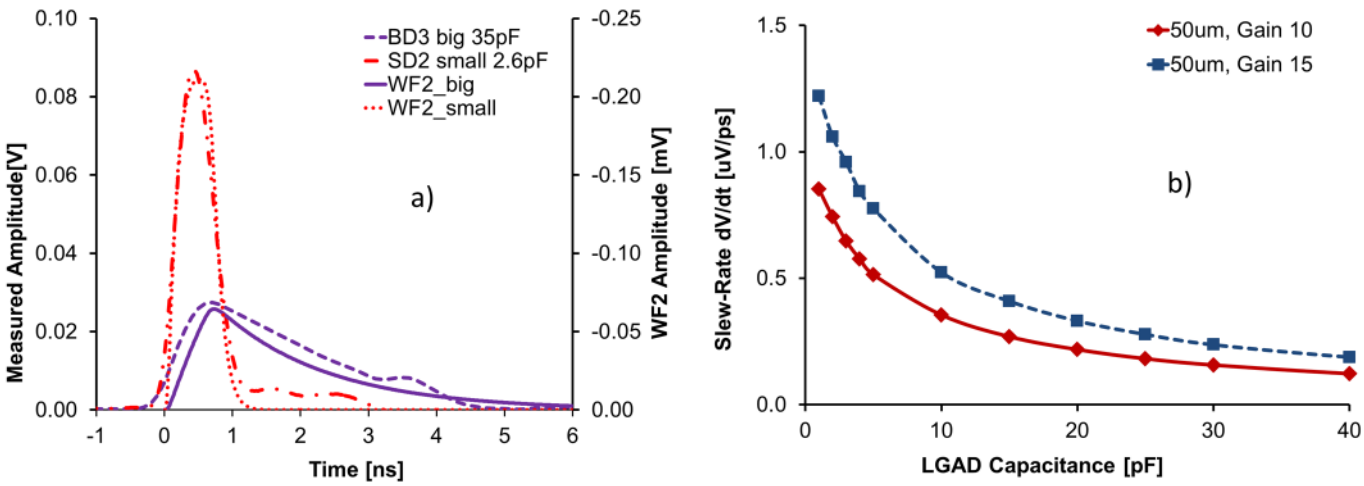

Fig. 9 Response to front α particle injection of 50 µm thick epitaxial LGADs: a) pulse shapes including WF2 simulations for different capacitances and gain of 3.5; b) slew-rate as a function of capacitance for LGAD with gain 10 and 15.

A second effect in the use of a broad-band amplifier is that the noise N is independent of the LGAD capacitance. We changed the capacitance between 2.6 and 223 pF by ramping up the bias voltage, and measured the RMS noise on random triggers using different low-pass bandwidth (BW) limits on the digital scope: as shown in Fig. 10 the noise RMS does not change over this large range of capacitances. At the highest bias beyond 400V, an increase of noise due to the leakage current is observed. For all capacitances, the bandwidth dependence of the noise varies like $(BW)^{0.4}$. We find N(1GHz) = 18 µV at the amplifier input.

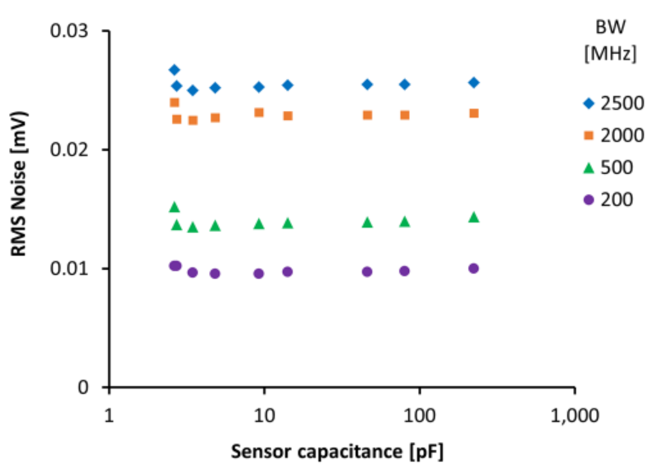

Fig. 10 Noise RMS of the SD2 epi LGAD for different Bandwidth limits when the capacitance is varied by changing the bias voltage.

The fact that the noise is independent of the capacitance allows us to calculate the time jitter, i.e. part of the timing resolution due to the noise, for different LGAD capacitances, by dividing the noise by the slew-rate (Fig. 9.b):

$$\sigma_{Jitter} = \left(\frac{N}{dV/dt}\right)$$

The time jitter vs. LGAD capacitance is shown in Fig. 11 for two noise values at the amplifier input: N = 18µV (presently measured) and N = 10µV (goal). A time jitter of 10 ps seems achievable for small capacitances, while the jitter for LGAD with C = 10pF can reach below 20 ps. As shown in Fig. 7, the time jitter constitutes the largest part of the time resolution. To set the scale, a 2mm x 2mm sensor, 50µm thick, has a capacitance of 8pF.

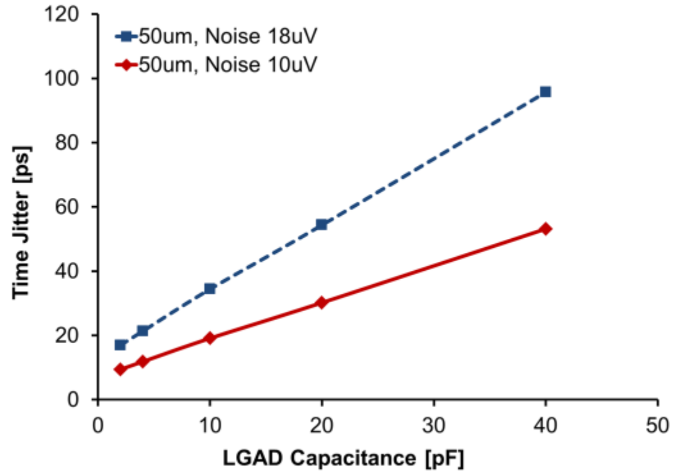

Fig. 11 Time jitter vs. LGAD capacitance for two noise values at the amplifier input: N = 18µV (presently measured) and N = 10µV (goal).

6 Conclusions

We measured the timing resolution of 300 µm thick Low-Gain Avalanche Diodes and found 120 ps in a beam test and 65 ps with an IR laser. Both numbers are in agreement with *Weightfield2* simulations. The same simulation program predicts a timing resolution of 30 ps for 50 µm thick LGAD of 2 pF capacitance.

Of the different methods used to determine the time stamp of a pulse, the constant-fraction discriminator shows the best performance.

We use 50 µm thick epitaxial LGAD with low gain to investigate the effects the sensor capacitance has on the pulse height and the slew-rate dV/dt, which is the main parameter determining the timing resolution of UFSD. When a broad-band amplifier is used, an increase of the capacitance from 2.6 pf to 35 pF decreases the pulse height by a factor 3 and the slew-rate by a factor 5.

With a broad-band readout, the LGAD noise is independent of sensor capacitance, and varies like $BW^{0.4}$ as a function of the band-width of a low-pass filter. Work to reduce the noise by a factor 2x beyond the presently achieved level is ongoing.

7 Acknowledgements

We thank HSTD10 Organizing Committee for their hospitality and the high scientific standards of the Symposium.

We acknowledge the expert contributions of the SCIPP technical staff. Part of this work has been performed within the framework of the CERN RD50 Collaboration.

The work was supported by the United States Department of Energy, grant DE-FG02-04ER41286. Part of this work has been financed by the Spanish Ministry of Economy and Competitiveness through the Particle Physics National Program (FPA2013-48308-C2-2-P and FPA2013-48387-C6-2-P), by the European Union's Horizon

2020 Research and Innovation funding program, under Grant Agreement no. 654168 (AIDA-2020), and by the Italian Ministero degli Affari Esteri and INFN Gruppo V.

8 References

[1] H. F.-W. Sadrozinski, "Exploring charge multiplication for fast timing with silicon sensors", 20th RD50 Workshop, Bari, Italy, June 2-6, 2012; https://indico.cern.ch/event/175330/session/8/contribution/18/attachments /225144/315064/RD50_Bari_UFSD_Sadrozinski.pdf.

[2] G. Pellegrini, *et al.*, "Technology developments and first measurements of Low Gain Avalanche Detectors (LGAD) for high energy physics applications", Nucl. Instrum. Meth. A765 (2014) 12.

[3] G. Pellegrini, *et al*., "Recent Technological Developments on LGAD and iLGAD Detectors for Tracking and Timing Applications" these Proceedings.

[4] H.F.-W. Sadrozinski, *et al*., "Sensors for ultra-fast silicon detectors", Nucl. Instrum. Meth. A765 (2014) 7.

[5] F. Cenna, *et al.*, "*Weightfield2*: A fast simulator for silicon and diamond solid state detector", Nucl. Instrum. Meth. A796 (2015) 149; http://personalpages.to.infn.it/~cartigli/Weightfield2/Main.html.

[6] B. Baldassari, *et al.*, "Signal formation in irradiated silicon detectors", 14th Vienna Conference on Instrumentation, Vienna, Austria, Feb. 15 -19, 2016.

[7] RD50 collaboration, http://rd50.web.cern.ch/rd50/.

[8] G. Kramberger, *et al.*, "Radiation effects in Low Gain Avalanche Detectors after hadron irradiations", 2015 JINST 10 P07006.

[9] G. Kramberger, *et al.*, "Effects of irradiation on LGAD devices with high excess current", 25th RD50 Workshop, CERN, Switzerland, Nov 19-21, 2014; Link: https://indico.cern.ch/event/334251/session/2/contribution/31/attachments/652609/897364 /Effect_of_excess_current_to_detector_operation.pdf25th RD50 Workshop, CERN, Switzerland, Nov 11-13, 2014.

[10] N. Cartiglia, *et al.*, "Design Optimization of Ultra-Fast Silicon Detectors", Nucl. Instrum. Meth. A796, (2015), 141–148.

[11] A. Seiden, "Ultra-Fast Silicon Detectors", PoS(VERTEX2015) 025, 2015.